



Fermi National Accelerator Laboratory

FERMILAB-Conf-83/101-THY
November 1983

Quarkonium : From the Bottom Up

Estia Eichten
Fermi National Accelerator Laboratory
P.O.Box 500
Batavia, Ill. 60510

and
Enrico Fermi Institute
University of Chicago
Chicago, Ill. 60637

Abstract

The status of quarkonium physics is reviewed. Emphasis is placed on what can be learned from detailed studies of the $b\bar{b}$ system about both the spin dependent and spin independent relativistic corrections to the static potential. Expectations for the $t\bar{t}$ system are briefly discussed.

Talk presented at the 1983 SLAC Summer Institute, Stanford, CA., July 18-29, 1983. To appear in the Proceedings of the SLAC Summer Institute on Particle Physics, Edited by P. McDonough.



2. The Explored Region - The Non Relativistic Potential

The effective potential between a heavy quark and a heavy antiquark can be defined in Q.C.D. (in the absence of light quarks) in terms of Wilson Loops. In general one can define the expectation values of any operator O in the presence of a Wilson Loop as:

$$\langle O \rangle = \frac{\int dA P \{ \exp[-g \int ds^\mu A_\mu^a t_a] \} e^{-S} O}{\int dA e^{-S}} \quad (1)$$

where P is the path ordering operator, S the pure gauge action, and C a closed rectangular path of length R in some space direction and length T in the time direction. The Static Energy is then given by

$$\epsilon(R) = \lim_{T \rightarrow \infty} -\frac{1}{T} \ln \langle 1 \rangle \quad (2)$$

A complete discussion of this formalism and the relation to the naive concept of a nonrelativistic potential appears in M. Peskin's Lectures in these Proceedings [2].

Some progress has been made recently in calculating $\epsilon(R)$ directly by using Monte Carlo Lattice Methods [3]. There is every expectation that this approach should give an accurate numerical determination of $\epsilon(R)$ within the next few years.

To date the only analytical calculations of the Static Energy have been in Q.C.D. perturbation theory and are therefore only valid for small R [4]. For $R \leq .1$ fm (Fermi) $\epsilon(R)$ is given by

$$R\epsilon(R) = -4/3 \alpha(R) + \text{order } \alpha^2 \quad (3)$$

where $\alpha(R) = \frac{12 \pi}{27 \ln(1/(RA))}$

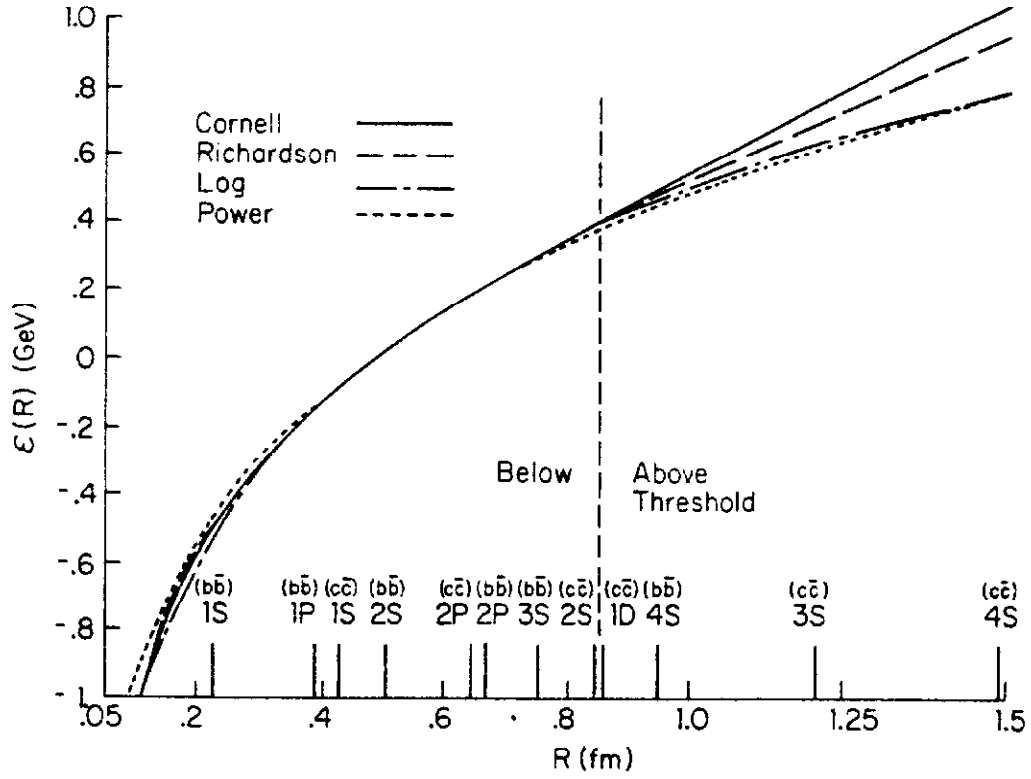


Figure 1: Phenemological Potentials for the $Q\bar{Q}$ System. The RMS radii of the observed $c\bar{c}$ and $b\bar{b}$ states are indicated by markers.

In the region of $R > .1$ fm many phenomenological potential have been proposed. Some of the simple alternatives are:

(1) Cornell Model [5]

$$\epsilon(R) = -\frac{\kappa}{R} + \frac{R}{a^2}$$

(2) Richardson Model [6]

$$\epsilon(R) = \int \frac{d^3 Q}{(2\pi)^3} e^{i\vec{Q} \cdot \vec{R}} \left[-\frac{4}{3} \frac{12\pi}{27} \frac{1}{Q^2 \ln[1+Q^2/\Lambda^2]} \right]$$

(3) Logarithmic Model [7]

$$\epsilon(R) = A \ln(R/R_0)$$

(4) Power Law Model [8]

$$\epsilon(R) = A (R/R_0)^\alpha$$

The first two models attempt to incorporate the expected behaviour of Q.C.D. at short distance ($\alpha(R)/R$) and long distance (αR) while the last two are motivated purely by the data. Fitting the parameters in these potentials to the $c \bar{c}$ system all do well in predicting the gross spectrum of the $b \bar{b}$ system. This is less surprising than it might first appear when one adds an overall constant to the potentials so that they all agree at $R = .4$ fm and then plots the potentials fitted to the $c \bar{c}$ system on the same figure. As seen in Figure 1, within the region $.1 \text{ fm} \leq R \leq 1.0 \text{ fm}$ all these potentials are in remarkable numerical agreement inspite of different analytic forms. Since the $\langle R^2 \rangle^{1/2}$ for all the $c \bar{c}$ and $b \bar{b}$ states below threshold for Zweig allowed decays is in this range of

R, the agreement for the predictions of these potentials is easily understood.

Another popular approach has been to use the inverse scattering method to determine the potential from the data itself [9]. The potential so determined agrees well with those in Figure 1. Furthermore, the potential constructed from the data in the $c\bar{c}$ system agrees well with that constructed from the $b\bar{b}$ system. This supports the Q.C.D. expectation of the flavor independence of the potential [10]. This flavor independence is particularly important in view of the prediction based on the Q.C.D. Sum Rule approach that potential models would fail for the masses in the $b\bar{b}$ system because of gluon condensate dependent effects [11]. Specifically, the C.O.G. (Center of Gravity) of the $1P$ ($b\bar{b}$) states is in good agreement with potential model predictions [12] and disagree with the prediction of the Q.C.D. Sum Rule approach [11].

To summarize the present situation with regard to the nonrelativistic potential for heavy quark antiquark systems:

(1). The potential is known very accurately in the range $.1 \text{ fm} \leq R \leq 1.0 \text{ fm}$. All the phenomenological potentials are essentially identical (numerically) in this region. Remaining differences in this range are small compared to the relativistic corrections which have not been incorporated in these analyses. I will discuss these corrections in the next two sections.

(2). For $R \leq .1 \text{ fm}$ the phenomenological potentials differ considerably, but Q.C.D. perturbation theory dictates the correct form. The toponium system (when discovered) will probe this small

distance region. I will discuss this further in Section 6.

(3). The flavor independence of the potential has been tested by the agreement of potentials fitted in the $c\bar{c}$ system with the spectrum of the $b\bar{b}$ system, and model independently by the inverse scattering method.

(4). We can conclude from (1),(2), and (3) above that the nonrelativistic potential (Static Energy) is well determined and flavor independent for $R \leq 1$ fm. However for distances greater than 1 fm the effects of open channels cannot be ignored (see Section 4). Thus a direct comparison of the spectrum with the predictions of the potential models is difficult. The Static Energy is certainly rising with R but the exact form can not be easily disentangled.

3. Spin Dependent Forces

As in the case of the potential itself, Q.C.D. dictates the form of the spin dependent forces. In particular the the spin dependent potentials can be expressed in terms of expectations in the presence of a Wilson Loop [13]. Using the notation of Eq. 1:

$$\begin{aligned}
 V_{\text{Spin Dependent}}(R) = & \left(\frac{S_1 \cdot L}{2m_1} + \frac{S_2 \cdot L}{2m_2} \right) \frac{1}{R} \left(\frac{d\epsilon(R)}{dR} + \frac{dV_1(R)}{dR} \right) \\
 & + \frac{(S_1 + S_2) \cdot L}{m_1 m_2} \frac{1}{R} \frac{dV_2(R)}{dR} + \frac{2}{3m_1 m_2} S_1 \cdot S_2 \nabla^2 V_2(R) \\
 & + \frac{1}{m_1 m_2} \left[S_1 \frac{R}{R} - S_2 \frac{R}{R} - \frac{1}{3} S_1 \cdot S_2 \cdot V_3(R) \right]
 \end{aligned} \tag{4}$$

where

$$\frac{R^k}{R} \frac{dV_1}{dR} = \epsilon^{ijk} \lim_{T \rightarrow \infty} \int_{-T/2}^{T/2} dt \int_{-T/2}^{T/2} dt' \frac{(t'-t)}{2T} g^2 \frac{\langle B^i(R,t) E^j(R,t) \rangle}{\langle 1 \rangle} \quad (5a)$$

$$\frac{R^k}{R} \frac{dV_2}{dR} = \epsilon^{ijk} \lim_{T \rightarrow \infty} \int_{-T/2}^{T/2} dt \int_{-T/2}^{T/2} dt' \frac{(t')}{2T} g^2 \frac{\langle B_i(0,t) E_j(R,t') \rangle}{\langle 1 \rangle} \quad (5b)$$

and

$$V_3(R) = -\frac{3}{2} \left(-\frac{R^i R^j}{R R} - \frac{1}{3} \delta^{ij} \right) \lim_{T \rightarrow \infty} \int_{-T/2}^{T/2} dt \int_{-T/2}^{T/2} dt' \frac{g^2}{T} \frac{\langle B_i(0,t) B_j(R,t') \rangle}{\langle 1 \rangle} \quad (5c)$$

In the future these correlations may be calculated directly by Monte Carlo Lattice methods. However, for now, the three potentials V_1, V_2 , and V_3 must be considered as unknown. It has been shown that an dhmmwneal general relation exists which follows from Q.C.D. alone [13]. For the case of equal mass quark and antiquark the unknown spin dependent potentials can be written:

(1) Spin Orbit Term - V_{so}

$$\frac{(S_1 + S_2) \cdot L}{2m} \left\{ -\frac{1}{R} \frac{d\epsilon}{dR} + V_{so} \right\} \quad (6a)$$

rcaoe

$$V_{so} = -\frac{1}{R} \frac{d(V_1 + V_2)}{dR}$$

(2) Tensor Term - V_t

$$-\frac{1}{3m} \left(3 S_1 \cdot \frac{R}{R} S_2 \cdot \frac{R}{R} - S_1 \cdot S_2 \right) V_t \quad (6b)$$

and

(3) Spin Spin Term - V_{ss}

$$\frac{2}{3m} \mathbf{S}_1 \cdot \mathbf{S}_2 V_{SS} \quad (6c)$$

where $V_{SS} = \nabla^2 V_2$

Many attempts have been made to model the potentials - V_{so} , V_t , and V_{ss} based on physical assumptions about the long or short range nature of these forces, their relation to the nonrelativistic potential, or analogies with Q.E.D. [13,14]. I will not consider any of these attempts here but will propose instead a simple purely phenomenological ansatz:

$$V(R) = A \left(R/R_0 \right)^\alpha \quad (7)$$

Thus each unknown potential has two parameters which describe the nature of the term. A gives a measure of the strength of the interaction ($R_0 = 1/\text{GeV}$) and α gives a measure of the range of the interaction.

First let me deal with the spin-spin interaction. The only experimental data for the hyperfine splittings is in the $c \bar{c}$ system [15]:

$$\begin{aligned} M(\Psi') - M(\eta_c') &= 111 \pm 5 \text{ MeV} \\ \text{and} \\ M(\Psi) - M(\eta_c) &= 92 \pm 5 \text{ MeV} \end{aligned}$$

The form of the spin-spin term has been calculated in perturbation theory [16]:

$$V_{SS}(R) = 4\pi \delta(R) \frac{4}{3} \alpha_{\overline{MS}}(m) \left\{ 1 + \alpha_{\overline{MS}}(m)/\pi \xi \right\} \quad (8)$$

where $\xi = 0.563 + 0.375 \left[\langle \ln(Q^2/m^2) \rangle_{NS} / |\phi_{NS}(0)|^2 \right]$

For a value of $\Lambda_{\overline{m}s} = .17$ GeV the measured spin splittings in the $c\overline{c}$ system agree well with the values obtained from Eq. 8. Hence there is no evidence for any long range contribution in the spin-spin force. Using the same value of $\Lambda_{\overline{m}s}$, the predicted value for the splitting $M(T) - M(\eta_c)$ is 30 GeV.

The situation for the spin-orbit and tensor forces is more complicated and confused. I will suggest a method of analysis which can help to clarify the situation.

The masses of spin triplet P states can be expressed as

$$\begin{aligned} M(^3P_2) &= M_0 + a + b - 2/5 c \\ M(^3P_1) &= M_0 - a - b + 2 c \\ M(^3P_0) &= M_0 - 2a - 2b - 4c \end{aligned} \quad (9)$$

where

$$a = \frac{1}{2m^2} \frac{1}{R} \langle \epsilon(R) \rangle \quad (10)$$

which is known in terms of the nonrelativistic potential. Hence the total spin orbit term $a+b$ has one piece (a) which is determined completely from the nonrelativistic potential and has a long range part. However the other piece

$$b = \frac{1}{2m^2} V_{so} \quad (11)$$

can not be derived from the nonrelativistic potential in a model independent way and therefore needs to be modeled phenomenologically. Similarly the tensor term

$$c = \frac{1}{3m^2} V_t \quad (12)$$

is not known in a model independent way.

The masses of the triplet $1P(c\bar{c})$ states have been measured to very high accuracy by the Crystal Ball collaboration [15]. The triplet $1P$ and $2P(b\bar{b})$ states have recently been measured by the CUSB Collaboration [18]. The masses of the 1^3P_2 and $1^3P_1(b\bar{b})$ states have been measured to high accuracy by the CLEO [17] and Crystal Ball [19] Collaborations. The present best values for these masses are given in Table 1.

3P_J (MeV)	$1P(c\bar{c})$ Ref. [15]	$1P(b\bar{b})$ Ref. [18]	$2P(b\bar{b})$ Ref. [18]
$J = 2$	$3,555.9 \pm 0.6$	$9,913.3 \pm 0.3 \left(\begin{smallmatrix} + \\ - \end{smallmatrix} 2 \right)$	$10,266.4 \pm 0.3 \left(\begin{smallmatrix} + \\ - \end{smallmatrix} 2 \right)$
$J = 1$	$3,510.0 \pm 0.6$	$9,893.6 \pm 0.4 \left(\begin{smallmatrix} + \\ - \end{smallmatrix} 3 \right)$	$10,249.3 \pm 0.4 \left(\begin{smallmatrix} + \\ - \end{smallmatrix} 3 \right)$
$J = 0$	$3,415.0 \pm 1.0$	$9,872.6 \pm 0.7 \left(\begin{smallmatrix} + \\ - \end{smallmatrix} 5 \right)$	$10,228.9 \pm 0.7 \left(\begin{smallmatrix} + \\ - \end{smallmatrix} 5 \right)$

Table 1: Masses of the Triplet P States in the $c\bar{c}$ and $b\bar{b}$ system.

Using this data we can determine the values of $(a+b)$ and c for each of these systems. The results are shown in Table 2.

	$1P(c\bar{c})$	$1P(b\bar{b})$	$2P(b\bar{b})$
$a + b$	$34.9 \pm .4$	11.7 ± 2.1	10.6 ± 2.1
c	$10.0 \pm .2$	1.55 ± 1.1	2.37 ± 1.1
a	20.14	7.5	5.6

Table 2: Values of the Spin Dependent Energies in MeV.

The values of a have been determined from theory using

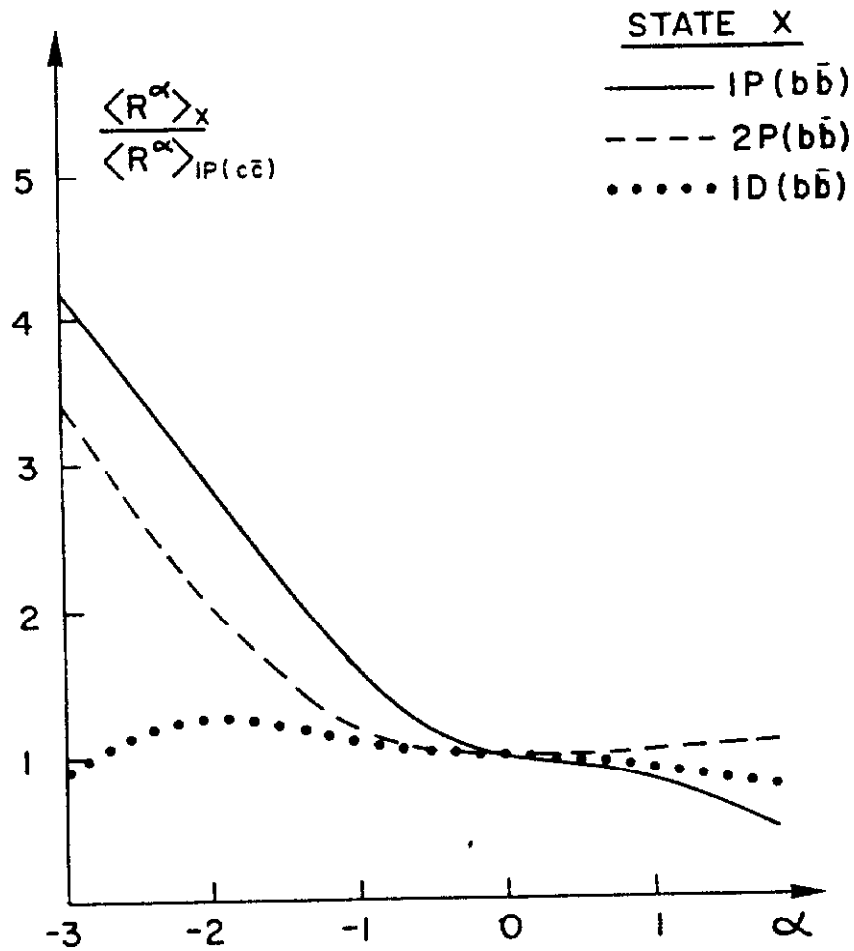


Figure 2: The Ratio of the Expectation Values of R^α in the State X to the Expectation Value of R^α in the $1P(c\bar{c})$ State. Expectation values are computed using the potential of Ref. [5].

the nonrelativistic potential determined in Section 2.

Now knowing the experimental values of b and c , we can determine in a model independent way some properties of the unknown part of the spin-orbit force and the tensor force. The present data for the P states in the $b\bar{b}$ system has rather large errors on the splittings so any conclusions we draw must be rather tentative; however I present this analysis to show the method and with the assurance that within the year the quality of the data will be such as to allow some firm conclusions.

The key to this analysis is that (as discussed in Section 2) the nonrelativistic potential is extremely well determined in the region of R (≤ 1 fm) relevant to our needs. Therefore the expectation of R in the various states of the $c\bar{c}$ and $b\bar{b}$ systems are known model independently. By the flavor independence of the spin dependent forces (true to leading order in v/c in Q.C.D.) the ratios

$$\frac{\langle R \rangle_X}{\langle R \rangle_Y} = \frac{\langle X|R|X \rangle}{\langle Y|R|Y \rangle} \quad (13)$$

where X and Y are any two states of these systems is a known function of a single variable α . The ratio is shown in Figure 2 for $Y = 1P$ ($c\bar{c}$) and various choices for X . Using the values of b and c from Table 2 and Eqs. (6b) and (6c) respectively we find that the experimental values for the ratios are:

X state	Spin Orbit Term - V_{so}	Tensor Term - V_t
1 P (b \bar{b})	$2.3 \begin{smallmatrix} + \\ - \end{smallmatrix} 1.1$	$1.22 \begin{smallmatrix} + \\ - \end{smallmatrix} .87$
2 P (b \bar{b})	$2.7 \begin{smallmatrix} + \\ - \end{smallmatrix} 1.2$	$1.87 \begin{smallmatrix} + \\ - \end{smallmatrix} .87$

Table 3: The Experimental Values of the Ratio $\langle R^\alpha \rangle_X / \langle R^\alpha \rangle_{1P(cc)}$
for the Potentials V_{so} and V_t for Various States X.

where the charm and bottom quark masses were choosen to be 1.84 GeV and 5.17 GeV respectively. Comparing these values with the ratios in Figure 2, we can read off the effective powers α of the spin dependent potentials determined by each of these ratios.

For the Spin Orbit Term (Eqs. 6b and 11):

$$\begin{aligned} \alpha &= -1.6 \begin{smallmatrix} + \\ - \end{smallmatrix} 1.0 & \text{for } X = 1 \text{ P (b } \bar{b}) \\ \alpha &= -2.5 \begin{smallmatrix} + \\ - \end{smallmatrix} 0.5 & \text{for } X = 2 \text{ P (b } \bar{b}) \end{aligned}$$

For the Tensor Term (Eqs.6c and 12):

$$\begin{aligned} \alpha &= -.8 \begin{smallmatrix} + \\ - \end{smallmatrix} 2.0 & \text{for } X = 1 \text{ P (b } \bar{b}) \\ \alpha &= -1.8 \begin{smallmatrix} + \\ - \end{smallmatrix} .8 & \text{for } X = 2 \text{ P (b } \bar{b}) \end{aligned}$$

Some tentative conclusions can be drawn for the V_{so} and V_t terms:

(1). The consistence of the method requires that the range determined from the two ratios ($X=1P$ and $X= 2P$) agree. Within the large experimental errors this is true.

(2). The expected behaviour of a short range potential is that of Q.C.D. perturbation theory

$$V_1(R) = \alpha(R)/R^3 \quad \text{i.e. } -3 < \alpha_1 < -2$$

while a long range spin potential should behave like $1/R$, i.e. $\alpha_1 = -1$. Thus the spin orbit potential $V_{so} (=V_1+V_2$ of Eq 6a) is consistent with being purely short range. This is not to surprising since we have already argued that the V_2 potential which also appears in the Spin-Spin force is consistent with perturbation theory, and the potential V_1 is zero both in perturbation theory and when instanton effects are included [13]. If better data supports the conclusion that V_{so} is short range then the whole spin orbit force would be calculable. The piece that contains a long range part (the a term) is determined directly from the nonrelativistic potential and the unknown piece (the b term) would be short range and so Q.C.D. perturbation theory should be a reliable guide.

(3). For the Tensor Term V_t (Eq.6c), the data suggests that there may be some long range component. The existence of a long range component of the tensor force has been suggested on phenomenological grounds by P. Moxhay and J. Rosner [21] and on theoretical grounds by J. Kogut and G. Parisi [22].

(4). Finally a word of caution about the analysis in the form I have presented. This analysis would be much more accurate if it could be performed without using any data from the $c\bar{c}$ system, since the $c\bar{c}$ system is surely more relativistic and hence the corrections associated with higher order effects and the light quark effects I will discuss in the next section are substantially larger. An analysis would be possible in the $b\bar{b}$ system alone if one addition spin splitting which involves the terms b and c could be measured. The best hope is to find the Triplet $1D$ ($b\bar{b}$) states. Ratios could

then be formed using $Y = 1D(b \bar{b})$. I will return to the feasibility of observing the $1D(b \bar{b})$ system in Section 5.

4. Spin Independent Relativistic Corrections

Many attempts to model the spin independent relativistic correction based on analogies with Q.E.D. have been made. These typically involve the reduction of the Bethe-Salpeter equation in the nonrelativistic limit with a kernel that is instantaneous and has some particular Lorentz structure. Two recent detailed treatments using somewhat different kernels have been presented. One approach (M+R) by P. Moxhay and J. Rosner [21] has a kernel with a long range potential ($\approx R$) which is a mixture of scalar and vector and has a long range tensor potential, and the other (M+B) by R. McClary and N. Byers [23] has a purely scalar long range potential. I will use these results in comparing theory with experiment in the photonic and hadronic transitions discussed in the next section. In this section, however, I would like to point out a serious shortcoming of these works and in fact all theoretical efforts to date which attempt to deal with the spin independent relativistic corrections to the potential.

There is an essential difference between Q.E.D. and Q.C.D. which first manifests itself in the leading spin independent corrections to the nonrelativistic limit. This is the effect of including light quark pair creation. Once we include light quark pairs the long range structure of the theory is drastically altered

in Q.C.D. since these terms allow the heavy quark and antiquark to be separated to infinite distance at finite energy. Each heavy quark is accompanied the associated light quark to form a color singlet meson. That is, the interactions of light quarks allow for strong (Zweig allowed) decays of the quarkonium systems above some kinematic threshold.

The inclusion of light quarks have the following practical consequences:

(1). The strict connection between the nonrelativistic potential and the Wilson Loop (or Static Energy) is lost. However, it is still formally valid to lowest order in the nonrelativistic expansion if we can argue that an expansion in inverse powers of the light quark effective mass is also possible. Although this seems improbable at first, I will argue below that this is probably numerically consistent.

(2). If the expansion suggested in (1) is valid for the potential itself it will also hold for to leading order for the spin dependent potentials as well. But there can be no justification for ignoring these terms when one considers the leading spin independent relativistic corrections. The light quark effects are at least as large as the leading spin independent corrections arising from an analysis based on the Bethe-Salpeter approach.

Unfortunately it is difficult to calculate the effects of light quark loops directly. Dealing with Fermion loops on the lattice is plagued with technical difficulties and a Monte Carlo calculation fully incorporating Fermion loops is still some time in the future.

However there is a phenomenological approach to including the effects of light quark loops. The approximate duality between using quarks and gluons as intermediate states and using the physical meson and baryon states suggests that for states near threshold for Zweig allowed decays the major effects of the light quarks will be included by including the coupling to decay channels in the manner of the Cornell Model [5]. This at least allows a rough estimate of the size of the light quark effects.

In Table 4 we compare the shift in masses due to coupling to decay channels and due to the relativistic corrections of the M+B model for various $c\bar{c}$ states below threshold. We conclude that the magnitude of these corrections are comparable. It is not possible to model the spin independent relativistic corrections without taking the light quark effects into account. The situation for the $b\bar{b}$ system is not better as is seen in Table 5.

I would also note the the magnitude of the light quark effect is considerably smaller than the energy differences between the states in the nonrelativistic limit which supports the assumption that an expansion in light quark mass as discussed in (1) above can be valid. The spin dependent shifts on the triplet $1P(c\bar{c})$ states has also been computed [5], they are +3 MeV, -3 MeV, and -1 MeV for the $J = 2, 1, 0$ states respectively. This supports the claim (2) above that the effects of light quarks can also be ignored for the leading order spin dependent forces.

In conclusion, although the effects of light quarks (or coupling to decay channels) can be reasonable ignored (in leading order) for the nonrelativistic potential and the spin dependent potentials, it is

State	M+B	C-C	Virtual $D \bar{D}$
ψ'	-117	-118	.20
$^3\chi_J(\text{C.O.G.})$	-55	-92	.12
ψ	—	-48	.04

Table 4: Mass Shifts in the $c \bar{c}$ System. The shift in mass due to the spin independent relativistic corrections of Ref. 23 are shown in Column M+B. The shift due to coupling to decay channels [5] is shown in Column C-C; while the probability for the wavefunction of the physical state to be a virtual $D \bar{D}$ state is shown in the last Column. All energies are in MeV.

State	M + B	C - C
Υ''	-56	-85
Υ'	-55	-50
Υ	—	-16

Table 5: Mass Shifts in the $b \bar{b}$ system. Notation as in Table 4.

not sensible to ignore these effects at the level of the leading spin independent relativistic corrections.

5. Transitions Among the Narrow $b \bar{b}$ States

Photonic Transitions

The only remaining puzzle in the $c \bar{c}$ system for the potential models, the disagreement of the calculations for the E1 photonic transitions for the 2S to 1P states, has been resolved. The results of McClary and N. Byers [23] are given in Table 6

$\Psi' \rightarrow \gamma \chi_J$	Naive Potential	Coupled Channel	McClary + Byer	Experiment
Rate in KeV	Ref. 5	Ref. 5	Ref. 23	Ref. 15
J = 2	29	23.7	22	$16.8^{+1.1}_{-1.1}$
J = 1	45	34	23	$19.1^{+1.1}_{-1.1}$
J = 0	50	43.2	16	$21.1^{+1.1}_{-1.1}$

Table 6: Successive Approximations to the 2S \rightarrow 1P E1 Transition

for the $c \bar{c}$ System.

The new ingredient in the calculation of M+B missing in the Cornell Coupled Channel Model [5] is the inclusion of the leading spin dependent and spin independent effects to the various states.

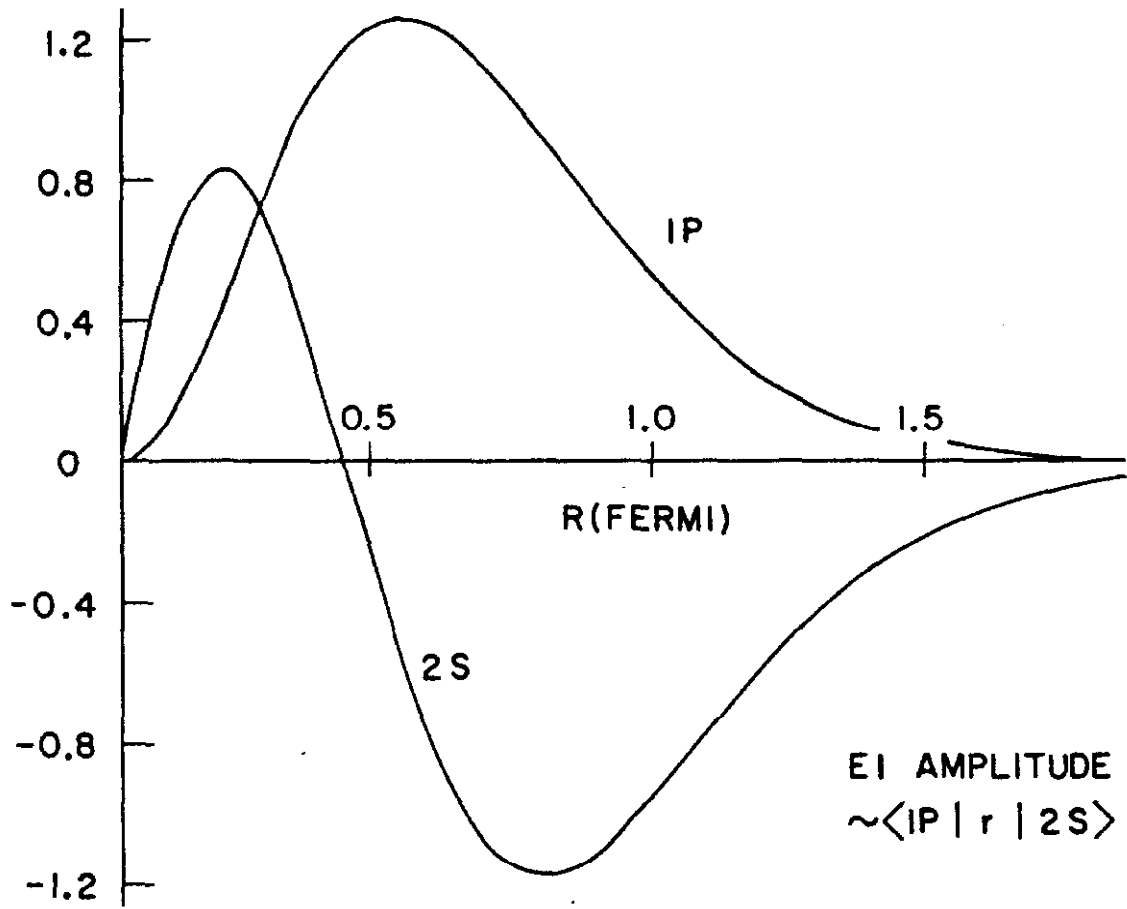


Figure 3: The Radial Wavefunctions for the $2\ ^3S_1$ (c \bar{c}) and $1\ ^3P_0$ States. The potential is given in Ref. [5].

Why are these relativistic effects so large when the nominal magnitude of these corrections should be $(v/c)^2 = .2$. The answer provided by the calculations of M + B that there is a strong cancellation in the overlap $\langle 2S | R | 1P \rangle$ which determines the E1 rate. This is due to the node in the 2S radial wavefunction as can be seen in Figure 3. Because of this cancellation the amplitude is particularly sensitive to higher order correction. The sign and relative magnitudes of the effect can be determined without any detailed calculations. The spin dependent terms will be strongly attractive for small R for the 1P J=0 state, neutral for the 1P J = 1 state, and repulsive for the 1P J =2 state; while the spin independent corrections (associated with kinetic energy corrections) will be attractive for all three 1P states. Hence the net effect is provide a strongly attractive term at short distance for the 1P J=0 state, a mildly attractive term for the 1P J=1 state, and an essentially neutral term for the 1P J=2 state. An attractive short range force will enhance the wavefunction of the state at short distance. Referring again to Figure 3 we see that enhancing the wavefunction of a 1P state at small R will increase the cancellation. This explains qualitatively the large effect seen in Table 6 for the J=0 1P state.

In general we may expect greater sensitivity to higher order correction whenever we have such cancellations. We should expect this in the b b system as well.

The spectrum of states below threshold for Zweig allowed decays in the b b system and the expected E1 and M1 transitions is shown in Figure 4. Transitions which would be expected to be sensitive to the

Transition	Theory	Experiment
$3S \rightarrow 2P_J \quad J=2,1,0$	11,12,6	13,16,3
$3S \rightarrow 1P_J \quad J=2,1,0$.6,.1,.1	seen
$2S \rightarrow 1P_J \quad J=2,1,0$	7,6,3	6,6,3
$2P_J \rightarrow 2S \quad J=2,1,0$	10,18,2	seen
$2P_J \rightarrow 1S \quad J=2,1,0$	9,15,1	seen
$1P_J \rightarrow 1S \quad J=2,1,0$	19,60,4	26,44,-
$2P_2 \rightarrow 1D_J \quad J=3,2,1$	1.4,3,-0	-
$2P_1 \rightarrow 1D_J \quad J=3,2,1$	0,2.5,2.2	-
$2P_0 \rightarrow 1D_J \quad J=3,2,1$	0,0,.8	-
$1^1P_1 \rightarrow 1^1S_0$	40	-

Table 7a: E1 Transitions in the $b\bar{b}$ System. The experimental branching ratios is taken from Ref. [20]. The theoretical rates are From Ref.[21]. Sensitivity to higher order relativistic effects is indicated in Figure 4. All branching ratios are in percent. Where not otherwise indicated the transition is between spin triplet states.

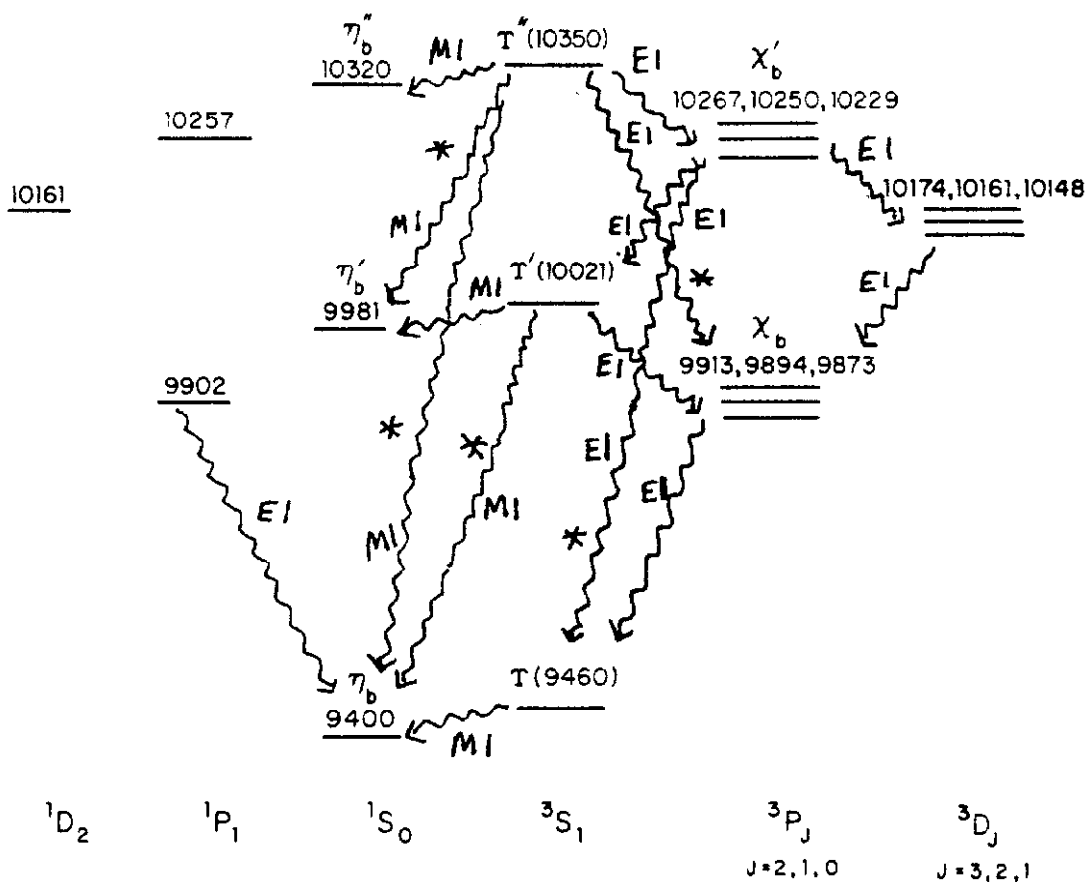


Figure 4: E1 and M1 Transitions in the $b\bar{b}$ System. Numbers above each set of states are the observed masses (in MeV) arranged in descending order of J . For states not yet observed the predicted masses (Ref. [13]) are indicated. Transitions which are particularly sensitive to relativistic corrections are indicated by a star.

Transition	Theory
$3^3S_1 \rightarrow 3^1S_0$	10^{-3}
$\rightarrow 2^1S_0$	10^{-4}
$\rightarrow 1^1S_0$	10^{-5}
$2^3S_1 \rightarrow 2^1S_0$	2.0×10^{-3}
$\rightarrow 1^1S_0$	10^{-2}
$1^3S_1 \rightarrow 1^1S_0$	2.0×10^{-2}

Table 7b: M1 Transitions in the $b \bar{b}$ System. Theoretical branching ratios are from Ref.[25]. The hindered M1 transitions are highly sensitive to the treatment of relativistic corrections. All entries are in percent.

treatment of higher order corrections are indicated with a star. The detailed comparison of the theoretical rates [21] and experiment is shown in Tables 7a and 7b.

Hadronic Transitions

The theory for hadronic transitions was discussed by M. Peskin in his lectures [2]. The basic idea is to make a multipole expansion for gluon radiation similar to the usual multipole expansion for photons. The expected hadronic transitions for the $b\bar{b}$ system are shown in Figure 5.

One difficulty is how to model the gluon to light hadron transitions. Kuang and Yan [24] have used a vibrating string model for the total rates for the transitions $n\ ^3S_1 \rightarrow m\ ^3S_1 + 2\pi$ and $n\ ^3S_1 \rightarrow m\ ^1S_0 + n$, while using free gluons projected onto into the right J^{PC} for all other transitions. Their results and a comparison with the present experimental rates is given in Table 8. For the shape of the spectrum in the $n\ ^3S_1 \rightarrow m\ ^3S_1 + 2\pi$ transition Kuang and Yan used soft pion theorems. The resulting shapes are in good agreement with the data for the $T'' \rightarrow T' + 2\pi$ and $T' \rightarrow T + 2\pi$ transitions, but give a poor fit to the spectrum shape in the case of the $T'' \rightarrow T + 2\pi$ transition in which the two pion system has the greatest energy (890 Mev). Whether the poor fit is just a result of a large extrapolation in two pion energy from the region of the soft pion theorems or a more basic problem with the hadronization model of Kuang and Yan is not known.

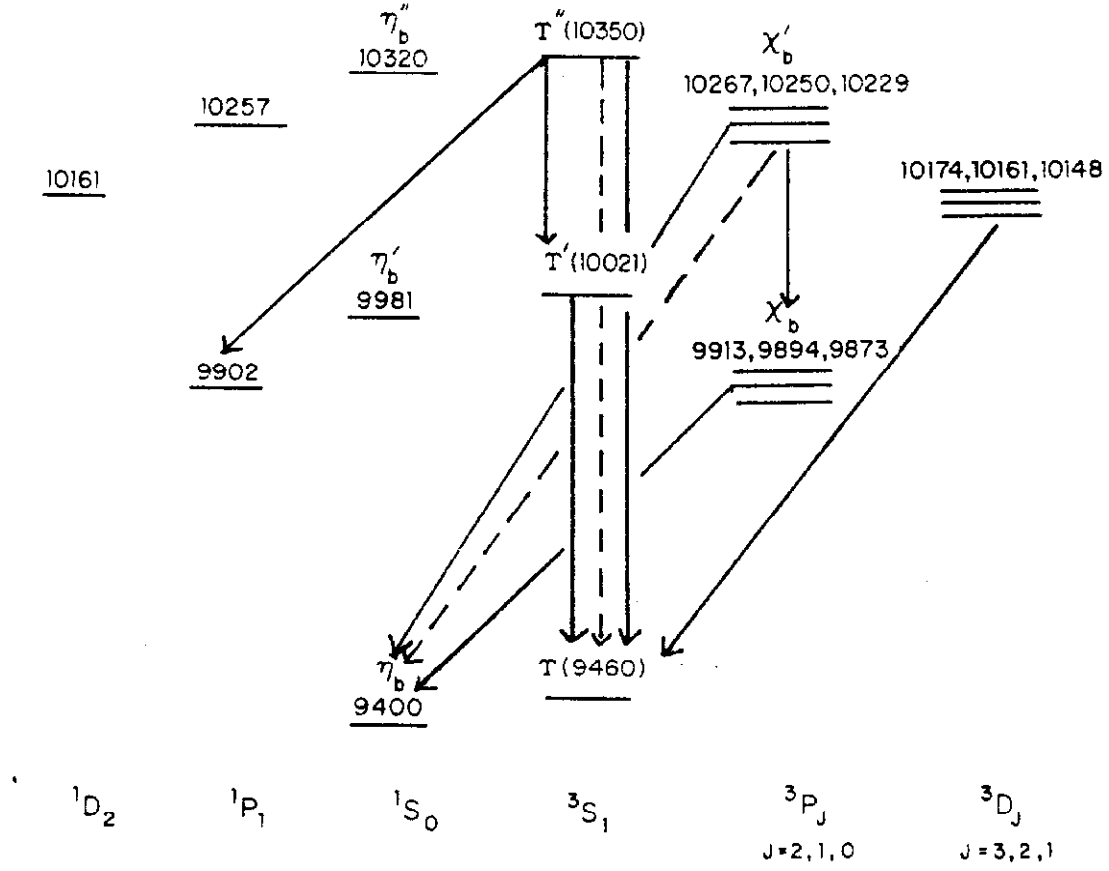


Figure 5: Some Hadronic Transitions in the $b\bar{B}$ System. A solid line denotes a 2π transition and a dashed line an π transition. The notation for the states is described in Figure 4.

Transition	Theory	Experiment
$3^3S_1 \rightarrow 2^3S_1 + 2 \pi$	2	5
$\quad \quad \rightarrow 1^3S_1 + 2 \pi$	5	7
$2^3S_1 \rightarrow 1^3S_1 + 2 \pi$	29	25
$2^3P_J \rightarrow \frac{2}{3} 1^3P_J + 2 \pi$.2, .3, .06	-
$2^3P_1 \rightarrow 1^1S_0 + 2 \pi$	2	-
$3^3S_1 \rightarrow 1^3S_1 + \eta$.03	-
$2^3S_1 \rightarrow 1^3S_1 + \eta$.04	-
$3^3S_1 \rightarrow 1^1P_1 + 2 \pi$.1	-

Table 8: Some Hadronic Transitions in the $b \bar{b}$ System. Experimental results are taken from Ref.[20]. Theoretical estimates based on the results of Ref.[24]. All branching ratios are in percents.

Observing Additional States in the $b\bar{b}$ System

We can use the predicted transition rates to determine which of the many additional states below threshold in the $b\bar{b}$ system can possibly be observed experimentally.

(1) The best available ways to observe the 3D_1 states is by the transitions

$$^3S_1 \rightarrow \gamma_1 + ^3P_J \rightarrow \gamma_1 + \gamma_2 + ^3D_{J'}$$

(a) For $J=2$ and $J'=3$, $\gamma_1 = 83$ MeV and $\gamma_2 = 93$ MeV

with a product branching ratio = .1%

(b) For $J=2$ and $J'=2$, $\gamma_2 = 106$ MeV

with a product branching ratio = .25%

(c) For $J=1$ and $J'=2$, $\gamma_1 = 100$ MeV and $\gamma_2 = 76$ MeV

with a product branching ratio = .5%

(d) For $J=1$ and $J'=1$, $\gamma_2 = 89$ MeV

with a product branching ratio = .4%

(2) The best way to see the 1P_1 state is through the hadronic transition $T'' \rightarrow ^1P_1 + 2\pi$ which has a branching ratio of .4 - .8 %. This rate is however highly dependent of the model of gluon hadronization [24].

(3) If the 1P_1 state is observed via (2) the state 1S_0 (η_b) can also be observed since the branching ratio for

$$^1P_1 \rightarrow ^1S_0 + \gamma \text{ with } \gamma = 502 \text{ MeV is approximately } 30\%.$$

(4) Unfortunately the M1 transition rates are uniformly tiny making observing the singlet S states impossible by these transitions. For example, the M1 transition $T \rightarrow \eta_b + \gamma$ with $\gamma = 50$ MeV has a branching ratio of approximately .06% [25]. However the transition

$$3^1S_1 \rightarrow \gamma + 2^3P_1 \rightarrow \gamma + 1^1S_0 + 2\pi$$

has a combined branching ratio of .3%. Hence the η_b may be observable by this mode.

6. Up from Bottom

The last remaining heavy quark system in the three generation model is the top system. We know from PETRA measurements [26] that the mass of the top quark must be greater than 19.3 GeV. If its mass is less than approximately 60 GeV it will be observed in W decays at SppS in the near future. What can we learn from toponium if the mass of the top quark lies in this range?

(1). There will be a rich spectrum of states below threshold. If we use a semiclassical argument [27] the number of S states are approximately $2(m_t/m_c)$. For $m_t = 30$ GeV there would be 8 S states below threshold and the maximum orbital angular momentum of a state below threshold would be 7; thus the total number of states below threshold would be approximately 45.

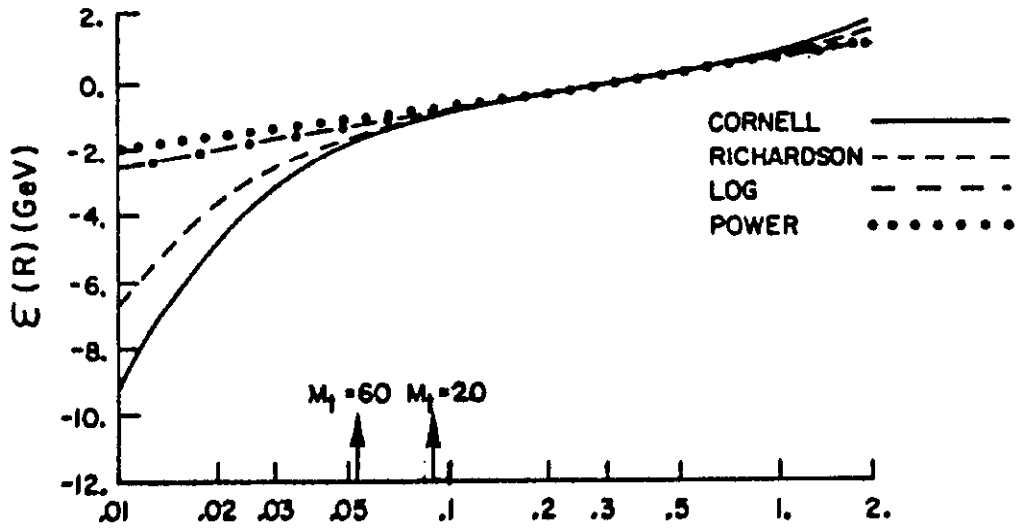


Figure 6: The Various $Q \bar{Q}$ Potentials of Figure 1 with their Short Distance Behaviour Displayed. The horizontal axis is the distance R in Fermi on a log scale. The markers indicate the radius of the $3S_1$ ($t \bar{t}$) state for $m_t = 20$ GeV and $m_t = 60$ GeV.

(2). We can probe the potential into smaller distances. As shown in Figure 6 the $\langle R^2 \rangle^{.5}$ for the 1S state is 0.09 fm for $m_t = 20$ GeV and .05 fm for $m_t = 60$ GeV. Thus we can test the perturbative Q.C.D. region of the potential. The difference between the 2S - 1S splitting in the Log and Q.C.D. inspired Richardson potential is shown in Table 9.

M(2S) - M(1S)	Top Quark Mass (Gev)				
	20	30	40	50	60
Log Potential	560	560	560	560	560
"Q.C.D."	587	610	630	645	660

Table 9: Dependence of 2S - 1S Splitting on the Top Quark Mass for Various Potentials. The Log potential is given in Ref. 7 and the "Q.C.D." potential in Ref. 6. All splittings are in Mev.

(3). The decays of the $t \bar{t}$ spin one ground state must include the full electroweak structure of the gauge interactions [28]. In particular we must include: (a) Virtual Electroweak term - photon and Z exchange in the s channel and W exchange in the t channel. (b) Weak t quark decays. (c) The three gluon annihilation term and (d) the two gluon plus photon term. The various decay rates are shown in Figure 7. Note that the three gluon annihilation no longer dominates these decays.

(4). If non standard models such as Technicolor or Supersymmetry are correct the ground state $t \bar{t}$ system could decay predominantly into new particles. For example, $1^3S_1 \rightarrow P^+ + b + t$ or $1^3S_1 \rightarrow \tilde{g} + \tilde{g}$.

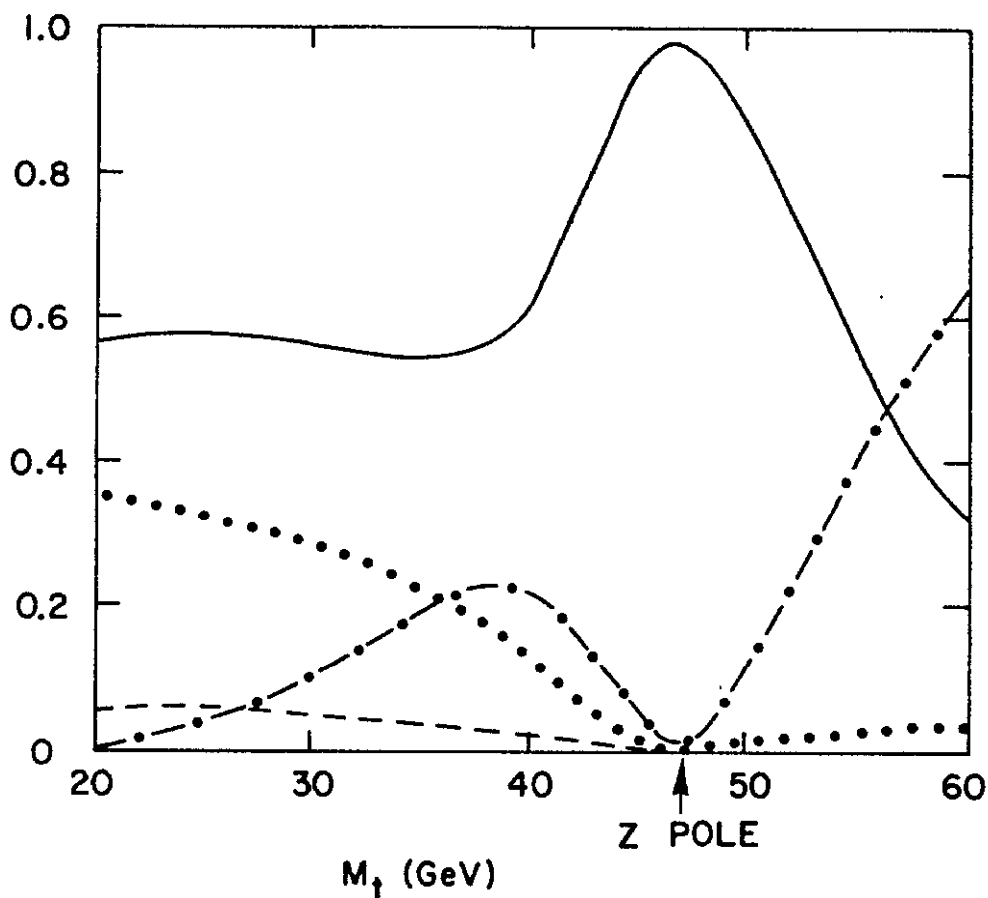


Figure 7: The Decay Branching Ratios for the $1^3S_1 (t \bar{t})$ State as a Function of Top Quark Mass. The solid curve is the contribution of the virtual Electroweak decays; the dotted curve the three gluon decays; the dot-dashed curve the W^+ weak t decays; and the dashed curve the two gluon -photon decays.

(5). Even if no unexpected decays dominate, accessing the rest of the spectrum with $L = 0$ through photonic or hadronic transitions from excited 3S_1 states will become extremely difficult for $m_t > m(Z_0)/2$. The expected branching ratios for direct decays, photonic transitions, and hadronic transitions is shown in Figure 8. The direct decays are as in (3) above. While for m_t in the range 20 - 60 GeV the photonic transitions satisfy the approximate scaling law $4 (m_b/m_t)^{2/3}$ from the corresponding state in the $b\bar{b}$ system. The hadronic transition rates scale according to Ref. [24].

7. Summary

In conclusion let me summarize the major results of our analysis of the status of Quarkonium Physics:

(1). The form of the nonrelativistic potential is established phenomenologically in the range $0.1 \leq R \leq 1.0$ fm. The next step is to derive this form from Q.C.D. For $R \leq 0.1$ fm the potential can be calculated in Q.C.D. perturbation theory; we need to confirm this form experimentally in the $t\bar{t}$ system.

(2). Leading order spin dependent relativistic corrections are in reasonable shape. The forms (range and strengths) of $V_{so}(R)$, $V_t(R)$, and $V_{ss}(R)$ will soon be known for experiment. The time will then be ripe for renewed model building for the spin dependent forces. Eventually these potentials will be calculated by lattice methods.

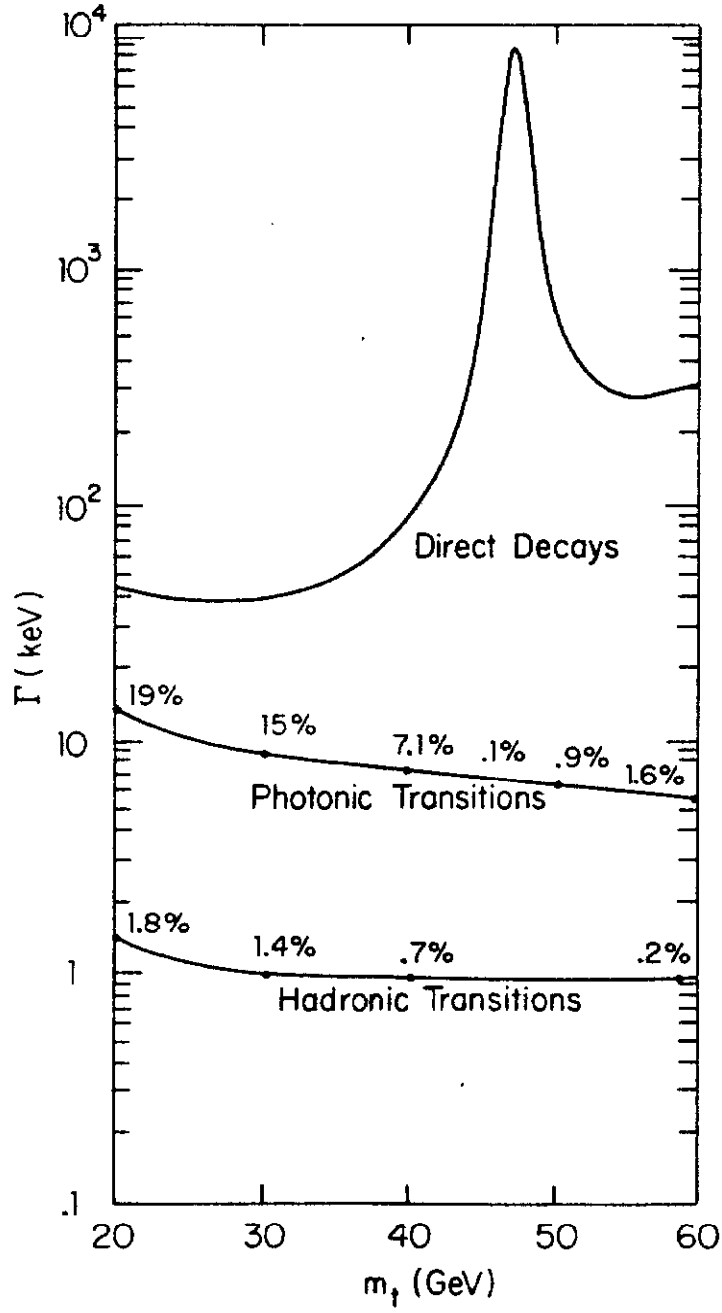


Figure 8: The Partial Widths of the Decays of the $3^3S_1 (t \bar{t})$ State.

(3). Spin independent relativistic corrections pose a very complicated problem. One can not ignore the effects of light quark loops (or equivalently coupling to decay channels).

(4). The theory of photonic transitions is in good agreement with the data. Care must be exercised when calculating rates to watch for E1 transitions which involve significant cancellation in the overlap integrals and for hindered M1 transitions, because these rates are more likely to be sensitive to higher order relativistic terms.

(5). The multipole expansion works well for hadronic transitions. It gives the correct scaling rules and overall rates. The hadronization of the gluons is not yet under theoretical control.

The $b\bar{b}$ system provides a rich spectrum of states in which to study the detailed structure of heavy quark systems. We are just beginning to learn this system. The $t\bar{t}$ system will provide an even richer spectrum and if $m_t \leq m(Z_0)$ we can look forward to one final system in which to study standard Quarkonium Physics.

References

1. For other reviews on the current status of Quarkonium Physics see: K. Gottfried, Rapporteur's talk given at International European Conference on High Energy Physics, Brighton, England, July, 1983; Cornell Preprint CLNS-83/579 (1983); and J. Rosner, "Progress in the Description Of Heavy Quark Systems", Enrico Fermi Institute Preprint EFI-83-17 (1983). I will not discuss the status of perturbative Q.C.D. applied to heavy quark systems. For a review of the situation in this field see: P. LePage, "Perturbative Q.C.D.", Summary talk presented at the International Symposium on Lepton and Photon Interactions at High Energies, Cornell University, Aug. 4-9 1983.

2. M. Peskin, Lectures presented at the 1983 SLAC Summer Institute. Published in the Proceedings of the 1983 Summer Institute On Particle Physics, Edited by P. McDonough, Stanford, CA.
3. For a review of the status of Lattice Monte Carlo methods for Q.C.D. see: J. Kuti, "Lattice Gauge Theories", Summary Talk at the International Symposium of Lepton and Photon Interaction at High Energies, Cornell University, Aug. 4-9, 1983.
4. This potential has been calculated through two loops by: F.L. Feinberg, Phys. Rev. Lett. 39, 316 (1977); T. Appelquist, M. Dine, and I. Muzinich, Phys. Lett. 69B, 231 (1977); and W. Fischler, Nucl. Phys. B129, 157 (1977).
5. E. Eichten et. al., Phys. Rev. D17, 3090 (1979); D21, 203 (1980).
6. J. Richardson, Phys. Lett. 82B, 272 (1979). For an extension of this model see: W. Buchmuller and S. H. H. Tye, Phys. Rev., D24, 132 (1981).
7. C. Quigg and J. Rosner, Phys. Lett. 71B, 153 (1977).
8. A. Martin, Phys. Lett. 93B, 338, (1980).
9. C. Quigg, H. B. Thacker, and J. Rosner, Phys. Rev. D18, 274 (1978); D18, 287 (1978); D21, 234 (1980).
10. C. Quigg and J. Rosner, Phys. Rev. D23, 2625 (1981).
11. M. A. Shifman, Proceedings of the 1981 Symposium on Lepton and Photon Interactions at High Energies, p.242 Ed. W. Pfeil, Bonn, (1981). Also see M. B. Voloshin, preprint ITEP-21 (1980).
12. See references 5 and 6 above.
13. E. Eichten and F. Feinberg, Phys. Rev. Lett. 43, 1205 (1979); Phys. Rev. D23, 2724 (1981).
14. W. Buchmuller, Phys. Letts. 112B, 479 (1982). also see references 21 and 23.
15. J. Gaizer, "Charmonium Spectroscopy From the Radiative Decays of the J/ψ and ψ' ", Ph. D. Thesis, Stanford University; SLAC-PUB 255 (1982).
16. W. Buchmuller, Y. J. Ng, and S. H. H. Tye, Phys. Rev., D24, 3003 (1981).
17. M. S. Alam et. al., Cornell Preprint Print 83-0869 (1983).
18. K. Han et.al., Phys. Rev. Lett. 49, 1612 (1982); G. Eigen et.al., Phys. Rev. Lett., 49, 1616 (1982); and C. Klopfenstein et.al., Phys. Rev. Lett., 51, 60 (1983).

19. J. Gaiser, "Results From The Crystal Ball at Doris II", Presented at the 11th SLAC Summer Institute on Particle Physics, Stanford, CA., July 18-29 (1983); SLAC-PUB-3223.
20. P. M. Tuts, "Heavy Quarkonia", Summary talk presented at the International Symposium on the Lepton and Photon interactions at High Energies, Cornell University, Aug 4-9 (1983).
21. P. Moxhay and J. Rosner, Phys. Rev. D28, 1132 (1983).
22. J. Kogut and G. Parisi, Phys. Rev. Lett. 47, 1089 (1981).
23. R. McClary and N. Byers, Phys. Rev. D28, 1692 (1983).
24. Y.P. Kuang and T. M. Yan, Phys. Rev. D24, 2874 (1981).
25. V. Zambetakis and N. Byers, "Magnetic Dipole Transitions in Onia", U.C.L.A. preprint UCLA/83/11 (1983).
26. B. Adeva et.al., Phys. Rev. Lett. 50, 799 (1983).
27. C. Quigg and J. Rosner, Phys. Letts. 72B, 462 (1978).
28. For details on decays including the Electroweak couplings see: J. H. Kuhn and K. H. Streng, Nucl. Phys. B198, 71 (1982).